EasyChair Preprint

№ 10640

Mechanical Properties of Plasticized Cellulose Acetate Magnesium Hydroxide Polypropylene Materials

Omar Al-Kubaisi, Aiping Yu, Hasan Majdi, Haidar Taofeeq and Christine Moresoli

July 31, 2023

Mechanical Properties of Plasticized Cellulose Acetate Magnesium Hydroxide Polypropylene Materials

Omar A-Kubaisi[1], Aiping Yu[2], Hasan Sh. Majdi[3], Haidar Taofeeq[4], and Christine Moresoli[2]

[1]Department of Chemical and Petrochemical Engineering, Faculty of Engineering, University of Anbar, Al-Anbar Governorate 31001, Iraq
[2]Department of Chemical Engineering, University of Waterloo, 200 University Avenue West, Waterloo N2L 3G1, Ontario, Canada
[3]Department of Chemical Engineering and Petrochemical Industries; Al- Mustaqbal University College, Babylon 51001; Iraq
[4]Chemical Engineering Department; College of Engineering; Al-Nahrian University; Baghdad; Iraq

July 27, 2023

Abstract

Plasticized cellulose acetate (CA*) and magnesium hydroxide (MH) were used as polymer blend and flame retardant, respectively, in polypropylene (PP). The mechanical properties, degree of crystallinity (X_c) and crystallization forms, were investigated. The results show that MH was well dispersed within the matrix with pure PP and PP*/CA* with neglected agglomeration. The blend and addition of CA* and MH deteriorated the tensile and impact strengths and improved Young's modulus of the PP materials. The degree of crystallinity (X_c) increased when MH and CA* were present, while CA* lowered the X_c measured by differential scanning calorimetry (DSC) and X-ray diffraction (XRD). DSC and XRD showed that CA* could induce β crystal for the PP material.

1 Introduction

The use of bio-composites for applications such as automotive components and building materials is increasing due to their ecological and economic considerations. Different organic fillers have been investigated, for example, wood fiber as reinforcement fillers [1], and cellulose derivatives [2] for polyolefin materials. It is generally believed that both flame retardant and mechanical properties are the most critical characteristics of bio-composite materials. In recent years, the flame retardation and thermal behavior of PP have been of growing interest.

PP is a semi-crystalline thermoplastic material with wide applications due to processability, mechanical properties, and chemical resistance at room temperature. PP has several polymorphs including the monoclinic α, trigonal β, and orthorhombic γ. The monoclinic α form is the most common and thermodynamically stable crystal form, predominating in normal processing conditions. The β form is metastable and is produced under defined crystallization conditions or in the presence of nucleating agents [3]. PP has been widely used in the fields of automobile, packaging, and so on. However, it has several disadvantages, such as molding shrinkage, low thermal deficiency temperature, and poor flammability resistance. These drawbacks make it unsuitable to use for many applications [4].

The viability of cellulosic fillers in thermoplastic materials has also been investigated in the literature. Composite materials containing cellulosic fillers represent a new class of materials that are relatively inexpensive. These fillers significantly display lower density than mineral materials. Moreover, reduced wear of the processing machinery could be considered as an advantage of using these fillers [2]. Previous studies have reported that the addition of cellulosic fillers reduces the strength and slightly reduces the impact strength of a composite material. The addition of cellulose to thermoplastic polymers, such as PP, yields a poor interfacial adhesion due to incompatibility-cellulose and PP are hydrophilic and hydrophobic, respectively [5]. Several pre-treatment methods, applied prior to the fabrication of composite materials, were reported for cellulose to improve its compatibility with polymer matrices [6–9]. Coupling agents and acetylation are the two main approaches used to improve such compatibility. The acetylation of cellulosic filler has been reported to improve the fiber matrix adhesion [10, 11]. Acetylation was reported by Luz et al. (2008), indicating that PP composite with acetylated fibers had a reduction in the tensile strength and intermediary thermal stability obtained for PP composites, i.e., the thermal stability of the composite is higher than neat fiber and lower than that of PP [12]. The authors stated that chemical modification did not contribute positively to the mechanical properties; hence, the composite reinforced with treated fibers showed the worst results (see Table 1).

Improvement in the flame retardancy is essential for them to meet safety requirements [13]. The most common flame retardant additives used are inorganic, halogenated, and phosphorus compounds. However, some flame retardant additives may cause negative health and environmental outcomes. Increasingly, attention is being paid to inorganic compounds such as metallic hydroxide additives (e.g., MH) instead [14, 15]. The introduction of particulate mineral fillers into the thermoplastic polymer can improve some mechanical properties, such as Young's Modulus or the heat deflection temperature, but may negatively affect other properties, such as the impact strength [16]. According to Das et al. (2017), the addition of MH improves the tensile moduli of PP composites but reduces their tensile strength because of the higher MH loading, which has been confirmed by other studies [17, 18].

The physical and mechanical properties of PP composites depend on the crystalline morphology and degree of crystallinity of the PP substrate. Investigations of the crystallization process of semi-crystalline polymers are of great importance in polymer processing. The mechanical properties of semi-crystalline polymers are mainly dependent on the nature of the crystal phase, crystallinity, and spherulite size [19]. The degree of crystallinity of PP may be affected by the inclusion of fillers and additives to the matrix as reported by different studies [20]. Fillers and additives have the potential to modify the crystallization characteristics of the polymer matrix depending on their density. Zhang et al. (2007) [21] studied the effects of carbon fiber loading on the morphology and melting behavior of PP and found that the morphology and crystallization characteristics of PP composites were strongly affected by the addition of short carbon. In a different study, XRD was used to evaluate the degree of crystallinity (X_c) of PP and PP/lignocellulosic composites. It was observed that the degree of crystallinity in the composites increased [22].

In this chapter, the mechanical properties of CA*/MH/PP bio-composite materials are presented and discussed. The mechanical properties were related to the morphology and crystallization characteristics. The degree of crystallinity obtained by DSC and XRD is also discussed.

Table 1: Published mechanical properties of PP and its composites

Composite	Tensile Modulus (GPa)	Tensile Strength (MPa)	Elongation (%)	Impact strength ($J \cdot m^{-1}$)	Reference
PP	0.51	31.6	>200%	-	[14]
PP/20 Cellulose	-	25.8(0.3)	6(0.3)		
PP/20Acetylated cellulose	-	20.1(0.4)	-	-	[12]
PP/30Cellulose	0.88(0.1)	23.7	9.8	-	[5]
PP/30MH	-	27.9	4.7	2.2	[23]
PP/30Sisal/40MH	2.36	28	-	-	[17]

2 Experimental methods

2.1 Materials

Fine PP powder (HM20/70P), purchased from GOONVEAN Fibres Company, was used as the polymer matrix. CA (approx. 50000 $g \cdot mol^{-1}$ 39% acetyl), MH, TEC, and PPMA were acquired from Sigma –Aldrich Company, Missouri, United States.

2.2 Materials preparation

Cellulose acetate (CA) was plasticized according to the methodology presented in Chapter 3.

Polypropylene (PP) materials were produced by extrusion in a twin screw-extruder (SJSZ-7A), Wuhan Ruiming Plastic Machinery Company, China. The four temperature zones ranged from 160 °C- 180 °C, and the circulation time was five minutes. The extruded materials were pelletized, and compression molded into tensile and impact specimens using and injection-molding machine (SZS- 20, China) and compression molding (PHI, Pasadena Hydraulic Inc., USA) at 200 °C with 10 bar pressure for 2 minutes. Table 2 lists the composition of the PP materials produced. PPMA was used in the fabrication of the as 3 wt.% replacement portion from the PP.

2.3 Tensile strength (ASTM D638)

The mechanical properties of the PP materials were measured at room temperature using an INSTRON 4465 tensile tester with a strain rate of 6 $mm \cdot min^{-1}$. The samples were kept at 23 °C and 50 % relative humidity for not less than 40. Five samples of each material were tested. The reported flexural strength is the maximum point of the stress/strain curve. Young's modulus represents the slope of the first linear part of the stress /strain curve. The sample size and dimension as shown in Figure 1.

Table 2: Sample composition and coding of PP materials

Material	PP wt.%	CA* wt.%	MH wt.%	PPMA wt.%
PP	100	0	0	0
PP*	97	0	0	3
60PP*/40CA*	58.2	40	0	1.8
70PP*/30MH	67.9	0	30	2.1
70(60PP*/40CA*)/30MH	40.74	28	30	1.26

PP* refers to 97PP /3PPMA.

CA* refers to plasticized cellulose acetate with triethyl citrate.

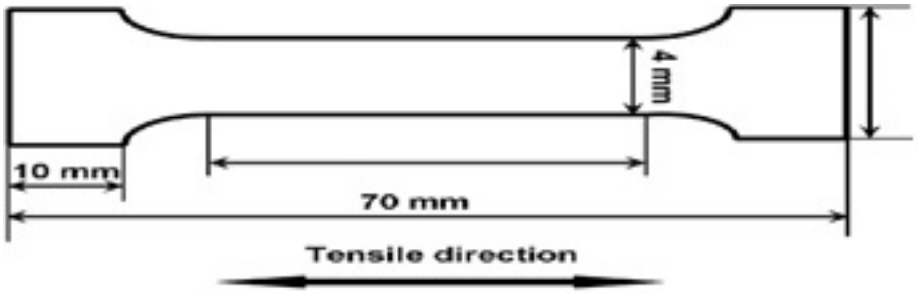

Figure 1: Tensile test specimen size and shape

2.4 Notched Izod impact test (ASTM D256)

The impact strength of the PP materials was measured with the Impact Test machine from Zwick/Roell (B5113.3), Germany at room temperature and a hammer work of 5.41 J. The test was conducted in the Quantum-Nano Centre at the University of Waterloo. The samples were kept at 23 ^{o}C and 50% relative humidity for not less than 40. Five samples of each material with size (60 mm$\times$10 mm$\times$3 mm) were tested.

2.5 Scanning electron microscopy

The morphology of PP materials was observed using a scanning electron microscope (SEM) (Quanta FEG 250). Rectangular-shaped samples (6 cm$\times$1.5 cm$\times$0.5 cm) were frozen in liquid nitrogen and cryofractured. In order to avoid charging, all surfaces were coated with a thin layer of gold. Elemental mapping was performed using Energy Dispersive Spectroscopy (EDS) in the equipment.

2.6 Differential scanning calorimetry (DSC)

The crystallization kinetics of PP materials was investigated with a Q2000 TA instrument (USA) calibrated by indium and sapphire disk standards, using standard T -zero. Nitrogen with a 50 ml$\cdot$min^{-1} flowrate

was used as purge gas. Samples of approximately 5-6 mg of the extruded materials as pellets were placed in an aluminum pan. The samples first were heated from room temperature to 200 °C at a heating rate of 10 °C·min^{-1}, and then maintained at this temperature for 5 minutes to remove previous thermal history. The samples were then cooled to 25 °C at different cooling rates (5, 10, 20, and 30 °C·min^{-1}). The heat flow was recorded as a function of temperature and time.

2.7 Wide angle X-ray diffraction (WAXRD)

The crystalline structure of PP materials were analyzed by wide angle X-ray diffraction. The sample was laid on the sample holder and analyzed with CuKα radiation (λ=1.54 Å) generated at a voltage of 45 kV and tube current of 35 A. The X-ray diffraction patterns were recorded in a 2θ angle. The range was from 5° to 80° and scan step size was 0.004° under continuous scan type. The degree of crystallinity was estimated as the ratio of the crystalline area to the total area under the diffraction peaks. Data analyses were performed using Origin -Pro software.

3 Results and discussion

3.1 Mechanical properties

3.1.1 Tensile strength

The tensile test provides the material's response to stress forces applied in the longitudinal part of the specimen. The tensile test properties of PP materials prepared with PPMA, MH, CA* are presented in Table 3.

The tensile strength of the PP materials decreased as the MH loading increased. At 95% confidence level, there was a significant decrease in the tensile strength of PP compared to 70PP*/30MH of 13%. However, tensile strength is not significantly influenced by MH except at high filler contents. It could be suggested that there is some degree of filler-matrix interaction at play; allowing the material to resist the imposition of tensile force [23]. According to previous studies, adding MH causes a reduction in the tensile strength and an elongation at break that could be attributed to the poor compatibility of MH and PP [24]. The tensile strength decreased when CA* was added to the PP matrix. This reduction was around 30% from the neat PP matrix. Luz et al. (2008) examined the chemical modification of cellulose by acetylation and its impacts on mechanical properties [12]. They reported that the tensile strength of PP with acetylated cellulose decreased. In their analysis of cellulose and other reinforcement fillers, they found that chemical modifications did not contribute to the mechanical properties. The combination of CA* and MH also decreased the tensile strength of the material by 30 %. The tensile strength and fracture toughness of polymer material depend on the interfacial adhesion between the filler and the polymer matrix [5, 25]. According to Griffith's theory, a significant agglomeration of particles in the polymer matrix creates a weak point which lowers the stress required for the material to fracture [26]. Other studies have found that the presence of fine particles dispersed within the polymer matrix makes plastic deformation easier; hence, lower tensile strength. When the fillers are well dispersed, the stress must be higher to propagate a micro-crack in the material. Furthermore, impact energy will largely be absorbed by plastic deformation occurring around the particle.

Table 3: Tensile test properties of PP materials(± standard error, n=5)

Material	Max. Load (kN)	Yieldstress (MPa)	Tensile strength (MPa)	Elongation At break(%)	Young Modulus (GPa)
PP	0.34	34.12 (± 3.8)	31.90 (± 5.3)	18.6	0.52 (± 0.01)
60PP*/40CA*	0.22	21.90 (± 3.)	$N.O.^a$	4.54	1.11 (± 0.61)
70PP*/30MH	0.3	29.90 (± 3.2)	29.60 (± 2.9)	7.33	0.64 (± 0.50)
70(60PP*/40CA*)/30MH	0.19	19.50 (± 1.5)	$N.O.^a$	2.22	1.41 (± 0.10)

a : *Not observed*

The modulus of elasticity which is measured by extending the initial linear portion of the load extension curve and dividing the difference in stress corresponding to any segment of a section on this straight line by the corresponding difference in the strain. The modulus of elasticity increased with CA* and MH (Table 7.3). Qiu et al. (2005) [5] reported the effects of cellulose on a PP matrix, Young's Modulus increases with the inclusion of cellulose. Similar results were obtained by Joseph et al. (2002) in a study of the effects of treated and untreated sisal fiber fillers [27]. The effect of MH was reported to have the same effect on the Young's Modulus of the PP matrix [28]. MH may block the movement of PP chains, increasing the stiffness of the material. The deformation of the specimen under tensile load would be difficult because MH provides structural rigidity to the polymer matrix [29]. The percolation theory [16] provides an alternative explanation for the increase in stiffness. This theory proposes that there is a concentration of stress in the region of the polymer matrix around each filler particle. If the distance between the filler particles is small enough, these zones will join during tensile loading and form a percolation network. This percolation network causes an increase in the elastic modulus of the material. When the particles are fine and well dispersed, the total effected volume is increased and the distance between particles is shorter; the percolation network develops more easily, and the modulus is thus increased [30].

The elongation at break decreased with CA* and with MH (Table 3). The addition of MH to the PP matrix reduced the elongation of the material by 50% compared to PP. The addition of CA* decreased the elongation by 70 %. The combination of CA* and MH caused a further reduction in the elongation of the material. The elongation at break was inferior to neat PP in all cases; therefore, the materials were rigid when compared to the matrix. Weak bonding between the fillers and matrix caused poor stress transfer when the samples were loaded with tension, leading to early rupture. Elongation at break, therefore, decreased in all test cases [12].

3.1.2 Impact strength

A notched impact test measures the energy during impact, i.e., the energy necessary to fracture a standard test piece [31]. The impact resistance decreased when CA* or MH were added to the matrix, as shown in Table 4. With a 95% confidence level, a significant difference was found in the impact test. The addition of CA* and MH to the matrix resulted in a 35 % and 80 % reduction, respectively.

Similar observations of the effect of MH on the impact strength of PP materials was also reported

Table 4: Impact test for PP materials (± standard error, n=5)

Materials	Impact Resistance /Notch Length ($J{\cdot}m^{-1}$)
PP	42.5 (± 1.20)
60PP*/40CA*	26.6 (± 4.00)
70PP*/30MH	8.7 (± 0.89)
70(60PP*/40CA*)/30MH	8.6 (± 0.80)

by Mai et al. [28]. They reported a significant reduction in the impact strength. This decrease in impact resistance can be attributed to the immobilization of PP chains, limiting their ability to adapt to deformation and hence making the materials more brittle [16]. Furthermore, each particle in the matrix can act as a micro-crack initiator because there is a weak filler/matrix interaction. When the interaction is weak, the interfacial layer cannot effectively transfer the stress [32].

3.2 DSC observation

Figure 2, thermograms are shown representing the non-isothermal crystallization process of PP materials. The thermal properties T_p, melting temperature T_m, heat of fusion, ΔH_m ($J{\cdot}g^{-1}$), and percentage crystallinity were obtained from DSC studies are presented in Table 5. The crystallinity of PP was determined as follows:

$$X_c(\%) = \frac{\Delta H_m}{\Delta H_m^o \times w} \times 100 \tag{1}$$

where ΔH_m^o (207 $J{\cdot}g^{-1}$) is the heat of fusion for 100% crystalline PP [33], ΔH_m ($J{\cdot}g^{-1}$) is the heat of fusion of the sample estimated from area under the melting peak of DSC curves, and w is the mass fraction of PP in the PP materials.

There was no significant change in the melting temperature of PP materials. The 70(60PP*/40CA*)/30MH had higher crystallinity than PP and the other materials. This could be another reason for the stiffness of this PP materials in comparison to the others.

3.3 Wide angle X-ray diffraction (WAXRD)

The XRD patterns of plasticized cellulose acetate (CA*) is given in Figure 3a. Two main broad peaks appear at 2θ of 9.0^o and 21.5^o. CA* shows a low degree of crystallinity (10%) due to plasticization effects. The XRD patterns of MH powder are given in Figure 3b. All peaks can be indexed as a hexagonal structure of MH with lattice constant [34]. The diffraction peaks of MH are at 2θ of 18.6^o, 38^o, 50.09^o, 58.7^o, 62.1^o, and 68.3^o with different intensities.

Figure 4 shows the diffraction patterns of PP materials. Several maxima can be observed. These peaks occur at 2θ values 14.5^o, 17.5^o, 19.1^o, 22^o and 22.5^o. The most intense are located at the 110, 040, 130, 111, and 041 planes, representing an α crystallization form. Similar results have been reported by Gupta and others [35–38]. For 60PP*/40CA*, the same peaks occur at a similar location, 2θ, with one extra

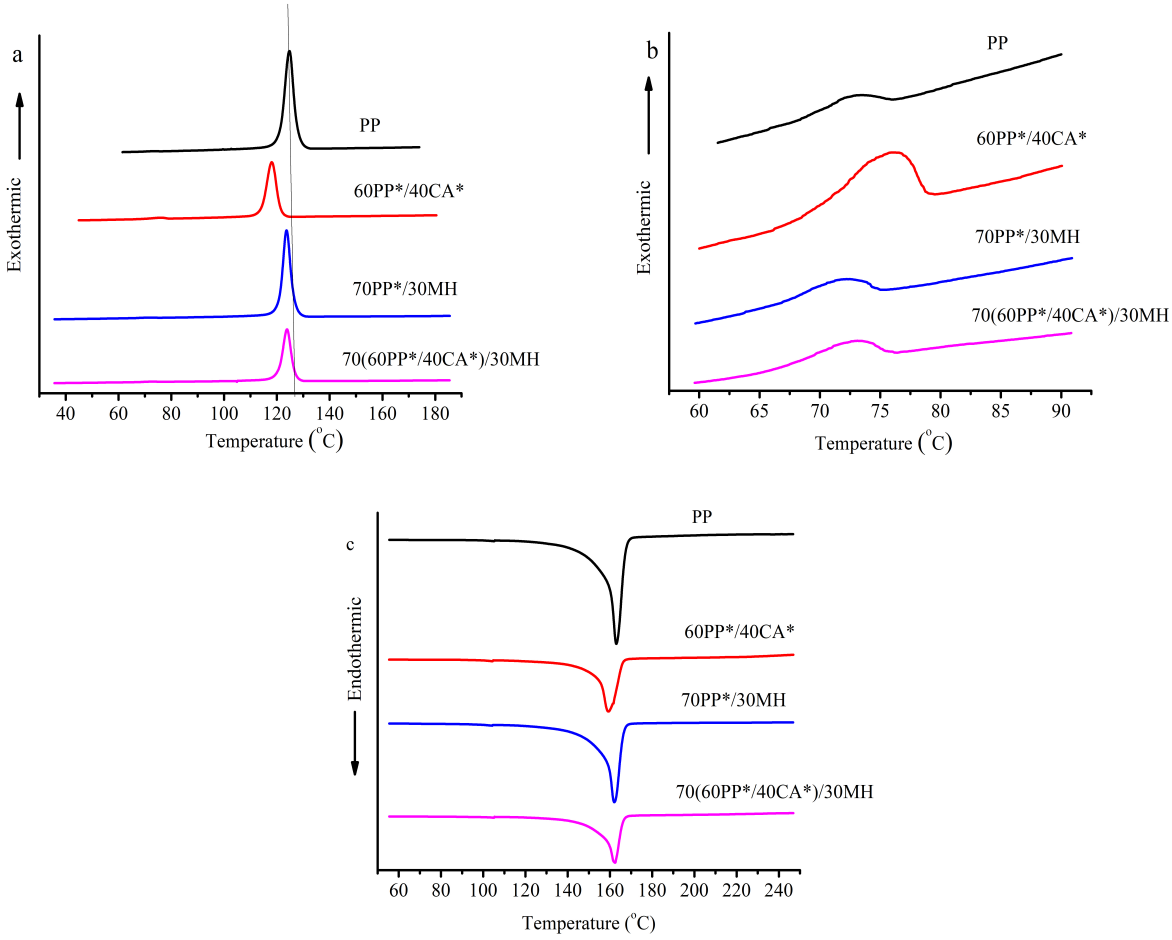

Figure 2: DSC thermograms of PP materials. a. crystal peaks, b.close β-crystal peaks, c.melting peaks

peak appearing at 16.5°. This could be related to β peak crystals with a reflection plane (300). This result also matches previous studies, which showed that a β crystal could be induced by adding other fillers or nucleating agents at the same 2θ [39, 40]. The decrease in peak intensity and peak broadening are smaller for the 60PP*/40CA* case than for the PP case, which could indicate that CA* increases the disorder of the PP structure. For 70PP*/30MH and 70(60PP*/40CA*)/30MH, the peaks are slightly shifted to lower angles, meaning that the distance between PP layers is increased. The intensity of these peaks is also reduced except for one; possibly related to the inclusion of MH. Moreover, the broadening of the peaks is also reduced for the 70(60PP*/40CA*)/30MH. The peak height and intensity could be affected by the variation in the spherulite size or their distribution, deformation at the spherulite boundaries, or the formation of the mesomorph phase of PP [35, 41].

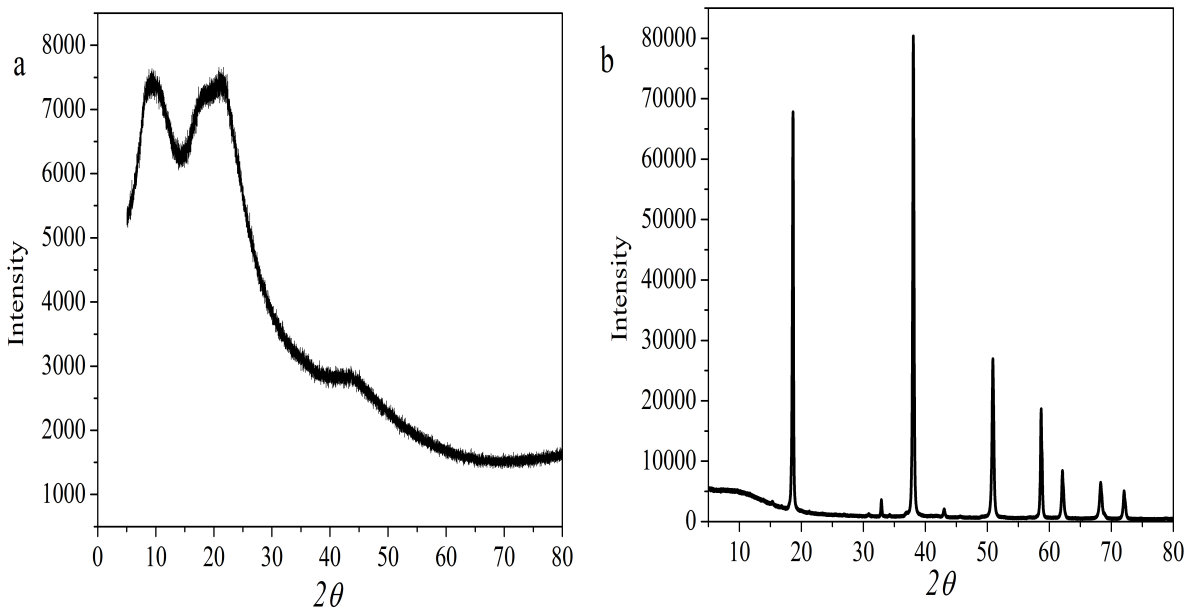

Figure 3: XRD patterns of a. plasticized cellulose acetate (CA*) and b. magnesium hydroxide (MH)

The degree of crystallinity (X_c) can be obtained from the following expression:

$$X_c(\%) = \frac{A_c}{A_a + A_c} \times 100 \tag{2}$$

where A_c is the crystalline area and A_a is the amorphous area in the XRD diffractograms.

The degree of crystallinity (X_c) of PP materials estimated from WAXRD diffractograms corresponds well with the degree of crystallinity obtained from DSC studies. Table 5 shows the degree of crystallinity calculated by XRD. Appendix **??** contains the baseline and area subtraction methods used for the amorphous and crystal region.

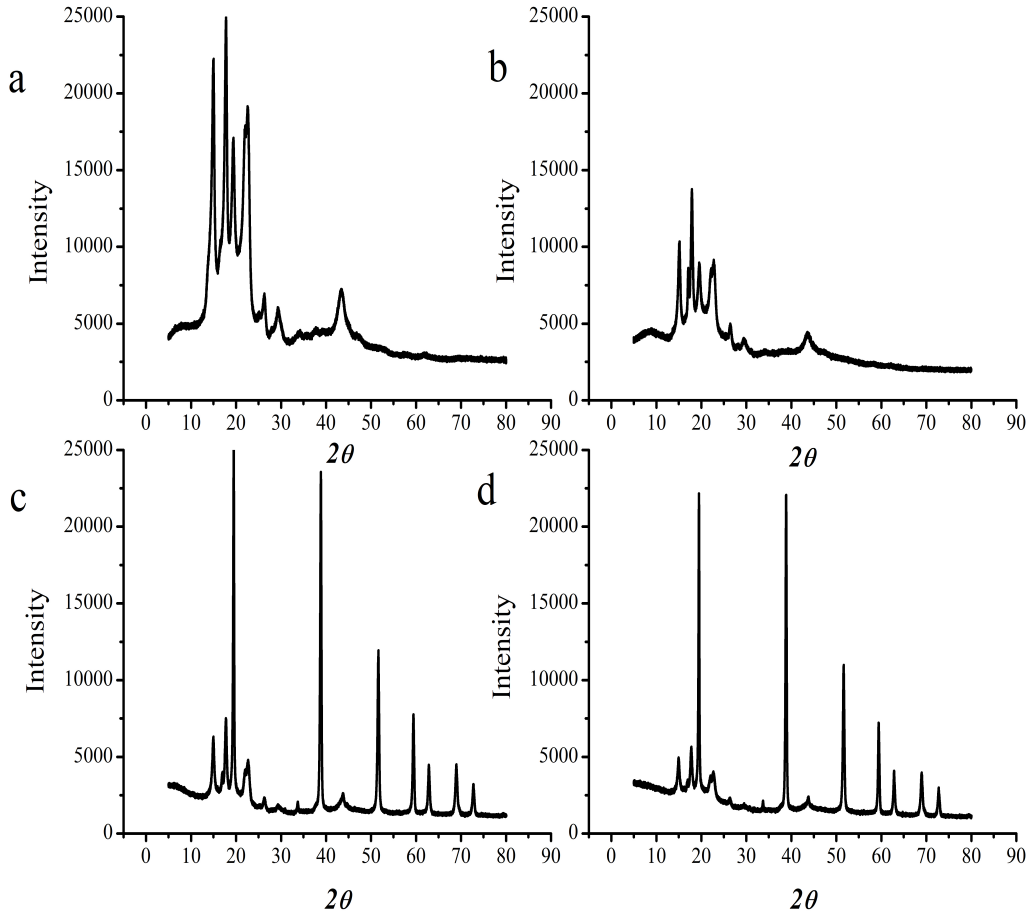

Figure 4: Comparison of the X-ray diffractograms of PP materials. a. PP, b. 60PP*/40 CA*, c. 70PP*/30 MH, and d. 70(60PP*/40CA*)/30MH

4 Conclusion

PP materials were fabricated by extrusion and injection or compression molding. The mechanical properties and crystallinity of the materials were evaluated.

The addition of MH markedly reduced the mechanical properties of PP materials. The notched impact strength reduction was larger than that for the tensile strength. From the observation of fractured surfaces,

Table 5: Thermal characteristics of PP materials

Material	T_m (^{o}C)	ΔH_m (J·g^{-1})	X_c(%) DSC	XRD
PP	163	85	46	47
60PP*/40CA*	159	48	43	42
70PP*/30MH	162	67	52	56
70(60PP*/40CA*)/30MH	162	42	54	58

it was revealed that extensive cracking and a lack of bonding at the filler/matrix interface were present. However, Young's modulus increased. A significant reduction in the tensile strength was observed after blending CA* with PP*; it was larger than the reduction caused by the addition of MH. In contrast, the reduction in impact strength was smaller than that of the material with MH added. CA* increased Young's modulus of MH. The presence of CA* and MH in the PP matrix reduced the tensile strength of the PP matrix, but a significant reduction was not observed in the impact strength in comparison to the 70PP*/30MH material. Young's modulus also increased in the combined CA* and MH.

The degree of crystallinity estimated by DSC and XRD showed that the PP material has a higher degree of crystallinity in the presence of MH and CA*-MH, while the blend of CA* reduced the degree of crystallinity. The inclusion of CA* induced β -crystal peak and had a favourable effect on the mechanical properties of PP.

In summary, the effects of MH on the mechanical properties and crystallization of the PP*/CA* have been reported for the first time in the literature. Further investigation is required on surface modification of MH to mitigate the reduction of the mechanical properties. The use of compatibilizer is also recommended to increase the compatibility between CA* and PP materials.

References

[1] M. Sain, S. Law, F. Suhara, and A. Boullinox. Stiffness correlation of natural fibre filled polypropylene composite. In *Proceedings of International Symposium on wood fibre plastic composites, France.*

[2] H. Dälvg, C. Klason, and H. E. Strömvall. The efficiency of cellulosic fillers in common thermoplastics. Part II. filling with processing aids and coupling agents. *International Journal of Polymeric Materials*, 11(1):9–38, 1985.

[3] R. Krache, R. Benavente, J. M. Lopez-Majada, J. M. Perena, M. L. Cerrada, and E. Pérez. Competition between α, β, and γ polymorphs in a β–nucleated metallocenic isotactic polypropylene. *Macromolecules*, 40(19):6871–6878, 2007.

[4] X. Chen, S. Zhang, G. Xu, X. Zhu, and W. Liu. Mechanical, flammability, and crystallization behavior of polypropylene composites reinforced by aramid fibers. *Journal of Applied Polymer Science*, 125(2): 1166–1175, 2012.

[5] W. Qiu, F. Zhang, T. Endo, and T. Hirotsu. Effect of maleated polypropylene on the performance of polypropylene/cellulose composite. *Polymer Composites*, 26(4):448–453, 2005.

[6] P. Anna, E. Zimonyi, A. Márton, A. Szép, S. Matkó, S. Keszei, G. Bertalan, and G. Marosi. Surface treated cellulose fibres in flame retarded PP composites. *Macromolecular Symposia*, 202(1):245–254, 2003.

[7] A. K. Bledzki and O. Faruk. Wood fibre reinforced polypropylene composites: Effect of fibre geometry and coupling agent on physico-mechanical properties. *Applied Composite Materials*, 10(6):365–379, 2003.

[8] G. Cantero, A. Arbelaiz, F. Mugika, A. Valea, and I. Mondragon. Mechanical behavior of wood/polypropylene composites: Effects of fibre treatments and ageing processes. *Journal of Reinforced Plastics and Composites*, 22(1):37–50, 2003.

[9] J. George, M. Sreekala, and S. Thomas. A review on interface modification and characterization of natural fiber reinforced plastic composites. *Polymer Engineering & Science*, 41(9):1471–1485, 2001.

[10] A. Paul, K. Joseph, and S. Thomas. Effect of surface treatments on the electrical properties of low-density polyethylene composites reinforced with short sisal fibers. *Composites Science and Technology*, 57(1):67–79, 1997.

[11] C. A. Willie Nelson, G. L. *Fire and polymers materials and solution for hazard prevention.* Oxford University Press, Washington, 2001.

[12] S. M. Luz, J. Del Tio, G. Rocha, A. Gonçalves, and A. Del'Arco Jr. Cellulose and cellulignin from sugarcane bagasse reinforced polypropylene composites: Effect of acetylation on mechanical and thermal properties. *Composites Part A: Applied Science and Manufacturing*, 39(9):1362–1369, 2008.

[13] M. Sain, S. H. Park, F. Suhara, and S. Law. Flame retardant and mechanical properties of natural fibre–pp composites containing magnesium hydroxide. *Polymer Degradation and Stability*, 83(2):363 – 367, 2004.

[14] O. Das, N. Kyeun Kim, A. L. Kalamkarov, A. K. Sarmah, and D. Bhattacharyya. Biochar to the rescue: Balancing the fire performance and mechanical properties of polypropylene composites. *Polymer Degradation and Stability*, 144:485–496, 2017.

[15] J. Z. Liang. Tensile and flexural properties of polypropylene composites filled with highly effective flame retardant magnesium hydroxide. *Polymer Testing*, 60:110–116, 2017.

[16] P. Mareri, S. Bastide, N. Binda, and A. Crespy. Mechanical behaviour of polypropylene composites containing fine mineral filler: effect of filler surface treatment. *Composites Science and Technology*, 58(5):747–752, 1998.

[17] R. Jeencham, N. Suppakarn, and K. Jarukumjorn. Effect of flame retardants on flame retardant, mechanical, and thermal properties of sisal fiber/polypropylene composites. *Composites Part B: Engineering*, 56:249–253, 2014.

[18] J. Z. Liang, J. Q. Feng, C. P. Tsui, C. Y. Tang, D. F. Liu, S. D. Zhang, and W. F. Huang. Mechanical properties and flame-retardant of PP/MRP/$Mg(OH)_2$/$Al(OH)_3$ composites. *Composites Part B: Engineering*, 71:74–81, 2015.

[19] P. Tordjeman, C. Robert, G. Marin, and P. Gerard. The effect of α, β crystalline structure on the mechanical properties of polypropylene. *The European Physical Journal E*, 4(4):459–465, 2001.

[20] N. G. Karsli and A. Aytac. Effects of maleated polypropylene on the morphology, thermal and mechanical properties of short carbon fiber reinforced polypropylene composites. *Materials & Design*, 32(7):4069–4073, 2011.

[21] Z. Zhou, S. Wang, L. Lu, Y. Zhang, and Y. Zhang. Isothermal crystallization kinetics of polypropylene with silane functionalized multi-walled carbon nanotubes. *Journal of Polymer Science Part B: Polymer Physics*, 45(13):1616–1624, 2007.

[22] E. Părpăriţă, R. Nicoleta Darie, Carmen-Mihaela Popescu, M. Azhar Uddin, and C. Vasile. Structure–morphology–mechanical properties relationship of some polypropylene/lignocellulosic composites. *Materials & Design*, 56:763–772, 2014.

[23] P. R. Hornsby and C. L. Watson. Interfacial modification of polypropylene composites filled with magnesium hydroxide. *Journal of Materials Science*, 30(21):5347–5355, 1995.

[24] X. Chen, J. Yu, and S. Guo. Structure and properties of polypropylene composites filled with magnesium hydroxide. *Journal of Applied Polymer Science*, 102(5):4943–4951, 2006.

[25] L. Nicolais and M. Narkis. Stress–strain behavior of styrene -acrylonitrile/glass -bead composities in the glassy region. *Composites*, 11(3):260., 1971.

[26] A. M. Riley, C. D. Paynter, P. M. McGenity, and J. M. Adams. Factors affecting the impact properties of mineral filled polypropylene. *Plastics and Rubber Processing and Applications*, 14(2):85–93, 1990.

[27] P. Joseph, K. Joseph, and S. Thomas. Short sisal fiber reinforced polypropylene composites: The role of interface modification on ultimate properties. *Composite Interfaces*, 9(2):171–205, 2002.

[28] Kan-cheng Mai, Y. Qiu, and Z. Lin. Mechanical properties of $Mg(OH)_2$/polypropylene composites modified by functionalized polypropylene. *Journal of Applied Polymer Science*, 88(9):2139–2147, 2003.

[29] J. Liang and Y. Zhang. A study of the flame–retardant properties of polypropylene/$Al(OH)_3$/$Mg(OH)_2$ composites. *Polymer International*, 59(4):539–542, 2010.

[30] D. He and B. Jiang. The elastic modulus of filled polymer composites. *Journal of Applied Polymer Science*, 49(4):617–621, 1993.

[31] J. F. Shackelford. *Stress versus strain*, page 155. Pearson Higher Education. Inc, Toronto, 2015.

[32] J. Z. Liang. Toughening and reinforcing in rigid inorganic particulate filled poly(propylene): A review. *Journal of Applied Polymer Science*, 83(7):1547–1555, 2002.

[33] R. L. Blaine. Determination of polymer crystallinity by DSC. *TA Instruments, New Castle, DE*, 2013.

[34] X. Chen, J. Yu, S. Guo, Z. Luo, and M. He. Effects of magnesium hydroxide and its surface modification on crystallization and rheological behaviors of polypropylene. *Polymer Composites*, 30(7): 941–947, 2009.

[35] A. K. Gupta and S. N. Purwar. Crystallization of PP in PP/SEBS blends and its correlation with tensile properties. *Journal of Applied Polymer Science*, 29(5):1595–1609, 1984.

[36] Z. Zhou, S. Wang, L. Lu, Y. Zhang, and Y. Zhang. Isothermal crystallization kinetics of polypropylene with silane functionalized multi-walled carbon nanotubes. *Journal of Polymer Science Part B: Polymer Physics*, 45(13):1616–1624, 2007.

[37] A. R. Bhattacharyya, T. V. Sreekumar, T. Liu, S. Kumar, L. M. Ericson, R. H. Hauge, and R. E. Smalley. Crystallization and orientation studies in polypropylene/single wall carbon nanotube composite. *Polymer*, 44(8):2373–2377, 2003.

[38] Y. Xu, Z. Sun, X. Chen, M. Chen, S. Hu, and Z. Zhang. Mechanical properties and crystallization behavior of polycarbonate/ polypropylene blends. *Journal of Macromolecular Science, Part B: Physics*, 52(5):716–725, 2013.

[39] R. P. Silva, V. Pistor, J. C. P. Vaghetti, and R. V. B. Oliveira. Influence of TiO_2 on the isothermal crystallization of polypropylene containing nanocomposites. *International Journal of Plastics Technology*, 20(1):67–78, 2016.

[40] Y. Zheng and Y. Chen. Preparation of polypropylene/Mg–Al layered double hydroxides nanocomposites through wet pan-milling: formation of a second-staging structure in LDHs intercalates. *RSC Advances*, 7(3):1520–1530, 2017.

[41] M. Modesti, A. Lorenzetti, D. Bon, and S. Besco. Effect of processing conditions on morphology and mechanical properties of compatibilized polypropylene nanocomposites. *Polymer*, 46(23):10237–10245, 2005.